ELSEVIER

Contents lists available at ScienceDirect

### Materials Today Chemistry

journal homepage: www.journals.elsevier.com/materials-today-chemistry/



## Ricinoleic acid as a reagent in the synthesis of ionomeric copoly (ester-amide)s for water soluble coating applications

Roberta L. de Paula <sup>a,2,1</sup>, Grazia Totaro <sup>a,3,1</sup>, Elisabete Frollini <sup>b,\*</sup>, Micaela Vannini <sup>a</sup>, Laura Sisti <sup>a,\*\*</sup>, Natália M. Inada <sup>c</sup>, Clara Maria Gonçalves de Faria <sup>c</sup>, Marianna Ciccone <sup>d</sup>, Francesca Patrignani <sup>d</sup>, Annamaria Celli <sup>b</sup>

#### ARTICLEINFO

# Keywords: Ricinoleic acid Castor oil Ionomers PET films Coatings Antimicrobial properties Poly(ester-amide)s

#### ABSTRACT

In this investigation, water-soluble coatings based on poly(ester-amide)s were applied to a commercial poly (ethylene terephthalate) (PET) film. In particular, poly(hexamethylene isophthalamide) (PA6I) was synthesized using 1,6-hexamethylene diamine (HMDA) and isophthalic acid (IPA). To impart water solubility to the material, 15 mol% of sulfonated groups was inserted along the macromolecular chain (PA6I/PA6ISO<sub>3</sub>). Additionally, 20 mol% of ricinoleic acid (RA) was introduced to potentially confer antimicrobial activity (PA6I/PA6ISO<sub>3</sub>/PRA). The PET-film coated with the prepared poly(ester-amide) shows potential for use in packaging and coating applications, particularly in the medical sector. The materials were characterized in terms of thermal properties by differential scanning calorimetry (DSC) and thermogravimetry (TGA), demonstrating high thermal stability and an amorphous nature. Mechanical properties were evaluated, and cytotoxicity tests were conducted using fibroblast cells. The results revealed significant improvements in elongation and strength at break compared to uncoated PET, suggesting good interfacial compatibility between the coating and the PET surface, as well as the absence of a toxic activity. Moreover, the presence of ricinoleic acid units conferred antibacterial activity, mainly against *Listeria monocytogenes*, a common foodborne pathogenic bacterium.

#### 1. Introduction

In recent years, concern over environmental issues has increased due to rising carbon emissions, deforestation, climate change, resource depletion, pollution, and waste accumulation in the environment [1]. As a result, researchers from both scientific community and industry have been seeking bio-based materials as alternatives to replace fossil-derived ones [2].

Poly(ester-amide)s (PEAs), which are copolymers combining the superior thermal and mechanical characteristics of polyamides with the

biocompatibility and biodegradability of polyesters [3] represent an interesting class of materials. They can be synthesized from renewable sources such as vegetable oils, which impart beneficial properties such as hydrophobicity, flexibility, and enhanced stability to the final product [4]. PEAs can also serve for example as polyols in polyurethane synthesis, yielding materials with high crosslinking density, excellent thermal stability, and high tensile strength [5]. Olive oil-based PEAs have been explored for biomedical applications [6] and for the development of resins with high thermal stability, chemical resistance, and biodegradability [7].

https://doi.org/10.1016/j.mtchem.2025.103147

Received 9 June 2025; Received in revised form 30 September 2025; Accepted 20 October 2025 Available online 30 October 2025

2468-5194/© 2025 The Authors. Published by Elsevier Ltd. This is an open access article under the CC BY-NC-ND license (http://creativecommons.org/licenses/by-nc-nd/4.0/).

<sup>&</sup>lt;sup>a</sup> Department of Civil, Chemical, Environmental and Materials Engineering, University of Bologna, Bologna, Italy

b Macromolecular Materials and Lignocellulosic Fibers Group, Center of Research on Science and Technology of BioResources, São Carlos Institute of Chemistry, University of São Paulo (USP), São Carlos, São Paulo, Brazil

<sup>&</sup>lt;sup>c</sup> Biophotonics Group, São Carlos Institute of Physics, University of São Paulo (USP), São Carlos, São Paulo, Brazil

d Department of Agricultural and Food Sciences, University of Bologna, Campus of Food Science, Cesena, Italy

<sup>\*</sup> Corresponding author.

<sup>\*\*</sup> Corresponding author.

E-mail addresses: elisabete@iqsc.usp.br (E. Frollini), laura.sisti@unibo.it (L. Sisti).

<sup>&</sup>lt;sup>1</sup> These Authors contributed equally.

<sup>&</sup>lt;sup>2</sup> Present address: Macromolecular Materials and Lignocellulosic Fibers Group, Center of Research on Science and Technology of BioResources, São Carlos Institute of Chemistry, University of São Paulo (USP), São Carlos, São Paulo, Brazil.

<sup>&</sup>lt;sup>3</sup> Present address: Department of Chemistry and Industrial Chemistry, University of Pisa, Via G. Moruzzi 13, Pisa, Italy.

The combination of polyesters and polyamides has great potential, since the advantages of both classes can be exploited to obtain materials for special applications, by finely tuning the monomer composition. For example, water-soluble polyamides are of particular interest because, in addition to generating materials with good mechanical, thermal, and anti-corrosion properties, they are also nontoxic and biocompatible. This makes them attractive for a wide range of applications, including water-based paints [8], water-based coatings and adhesives with good oxygen barrier properties [9], thermoplastic materials [10], and drug carriers [11].

A relatively unexplored, yet promising approach for producing water-soluble polyamides, is the random incorporation of ionic groups along the polymer chain. This modification enhances the polarity and hydrophilicity of the polymer [12–14]. A study by Vannini et al. focused on ionomeric polyamides: poly(hexamethylene isophthalamide) (PA6I), synthesized from 1,6-hexamethylenediamine and isophthalic acid, was used to produce films with exceptional thermal stability and excellent oxygen barrier properties. When 5-sulfoisophthalic acid (5-SIPA) sodium salt was added to the reaction mixture, an ionomeric polyamide was obtained. The introduction of ionic groups makes the sulfonated polyamides soluble in water, enabling their application as coatings and adhesives with favorable barrier properties [9].

To impart additional functionalities to water-soluble polyamides, ricinoleic acid (RA, or 12-hydroxy-9-octadecenoic acid), was explored in this study. RA is the major component of castor oil, which is obtained from the seeds of *Ricinus Communis* plant. It features three reaction sites: a carboxyl group, a double bond, and a hydroxyl group, offering wide possibilities for structural modification, which makes it very attractive for a variety of applications [15]. Moreover, its aliphatic side chain can interact with bacterial membranes, causing damage and/or disruption, thus exerting a biocidal effect [16,17]. The self-polycondensation of RA yields poly(ricinoleic acid) (PRA), a viscous liquid oligomer with low molar mass [16,17]. Copolymerization of RA further expand its range of application: for example, RA combined with sebacic acid has been studied for biomedical applications such as drug delivery systems [18-20]; RA has also been copolymerized with terephthalic and isophthalic acid to obtain materials with good mechanical properties and antibacterial activity, suitable for textile and engineering applications [17]. In addition, RA is used as a component in lubricants [21] and as flexible segment in polyurethanes, making them suitable for coatings and packaging [22]. Antibacterial electrospun membranes, useful in biomedical, food, and water/air filtration applications, have also been developed by blending PRA with poly(butylene succinate) (PBS) [23].

Based on these considerations, poly(ester-amide)s incorporating RA and ionomeric units were synthesized to develop water-soluble coatings with potential antibacterial properties. A commercial poly(ethylene terephthalate) (PET) film was chosen as support. PET is one of the most common and versatile plastics, widely used in bottles and films for packaging cosmetics, personal care products, and pharmaceuticals. Its wide use stems from its non-toxicity and ability to yield materials with excellent mechanical properties and strong O<sub>2</sub> and CO<sub>2</sub> barrier performance [24]. However, PET is relatively inert and hydrophobic, which favors bacterial adhesion and poses risks of infection in biomedical applications and implants. Furthermore, PET exhibits high static electrification, low wettability, and poor dyeability [25]. To overcome these limitations, surface modification strategies are under investigation, with polymer coatings standing out as one of the simplest and most cost-effective approaches [26,27].

In the present study, ionomeric copoly(ester-amide)s for water-soluble PET coatings were developed. The materials prepared included PA6I, derived from 1,6-hexamethylenediamine (HMDA) and isophthalic acid (IPA), together with its corresponding ionomeric copolymers synthesized using sodium 5-sulfoisophthalate (5-SIPA) and RA. The IPA/5-SIPA ratio was set at 80/20 (mol%), based on previous studies identifying this composition as suitable for films with low oxygen permeability and good water solubility, making them appropriate for coating

applications [9]. The ionomeric copolymer PA6I/PA6ISO $_3$ /PRA was prepared using the same PA6I/PA6ISO $_3$  ratio, with a molar composition of 64/16/20 for IPA, 5-SIPA, and RA, respectively.

Biaxially oriented PET films were coated with aqueous solutions of the synthesized copolymers  $PA6I/PA6ISO_3$  and  $PA6I/PA6ISO_3/PRA$ , after a corona treatment.

The synthesized materials were characterized using nuclear magnetic resonance (<sup>1</sup>H NMR) and thermal analyses (TGA and DSC). The coated PET films were further evaluated for tensile properties, cytotoxicity, and antibacterial activity.

The strategy adopted here shows strong potential for addressing several challenges in the development of water-soluble polymer coatings, including achieving adequate mechanical performance, ensuring biodegradability and sustainability, controlling adhesion and long-term stability, developing functional coatings that are simple to be applied, and overcoming the inherent trade-offs between water solubility and water resistance after application.

#### 2. Experimental section

#### 2.1. Materials

Isophthalic acid (IPA), 5-sulfoisophthalic acid sodium salt (5-SIPA), 1,6- hexamethylenediamine (HMDA), sodium hypophosphite, ricinoleic acid (RA, purity around 80 %), and titanium tetrabutoxide (TBT) were purchased from Sigma-Aldrich, while sodium acetate was supplied by Carlo Erba. All materials were of high purity and used as received. In the coating tests, biaxially oriented PET films (SARAFIL, 23  $\mu$ m thickness) supplied by POLIPLEX were used as the substrate.

#### 2.2. Syntheses of polymers and copolymers

All the syntheses were performed introducing reagents and catalyst into a 250 mL round, wide-neck glass reactor. The reactor was equipped with a three-necked flat flange lid, a heating band, a water-cooled condenser, a mechanical stirrer, and a torque meter to ensure precise control and monitoring. The reactor was placed in a 190 °C temperaturecontrolled salt bath and continuously stirred during the operation. The temperature settings for the heating band were tailored to the specific types of monomers being used. The first polymerization stage began with the distillation of any condensation products. Following this, the temperature was raised, and a heating band was used to maintain the lid at the same temperature. Next, in the second stage, a dynamic vacuum was applied, if necessary, and sustained until the polymer was released from the reactor. Table 1 lists acronyms and composition of the prepared polymers and copolymers while the respective reactions are depicted in Schemes 1-4. Further details for each polycondensation synthesis are provided below.

#### 2.2.1. Synthesis of the polyester: poly(ricinoleic acid)

Poly(ricinoleic acid) (PRA) was synthesized using the method

**Table 1**Acronyms and molar composition of polymers and copolymers.

		1 7		
Acronyms	Material	RA (mol %)	IPA (mol %)	5-SIPA (mol%)
PRA	Poly(ricinoleic acid)	100	0	0
PA6I	Poly(hexamethylene isophthalamide)	0	100	0
PA6I/ PA6ISO <sub>3</sub>	Poly(hexamethylene isophthalamide-co-5-sulfoisophthalamide)	0	80	20
PA6I/ PA6ISO <sub>3</sub> / PRA	Poly(hexamethylene isophtalamide-co-5-sulfoisophtalamide-co-ricinoleic acid)	20	64	16

Scheme 1. Synthesis of poly(ricinoleic acid) (PRA)

Scheme 2. Synthesis of poly(hexamethylene isophthalamide) (PA6I).

**Scheme 3.** Synthesis of ionomeric polyamide poly(hexamethylene isophthalamide-*co*-5-sulfoisophthalamide) (PA6I/PA6ISO<sub>3</sub>).

outlined by Totaro et al. [12]. The synthesis involved the addition of 42.00 g of ricinoleic acid and 0.049 g of TBT catalyst to the reactor (Scheme 1). The first stage lasted 2 h (T = 200  $^{\circ}$ C), followed by the second stage, which was maintained for 4 h and 45 min at 230  $^{\circ}$ C and 0.055 mbar after 1 h under a temperature and vacuum ramp. The resulting product discharged from the reactor was a liquid with low viscosity.

2.2.2. Syntheses of the polyamides: poly(hexamethylene isophthalamide) (PA6I) and poly(hexamethylene isophthalamide-co-5-sulfoisophthalamide) (PA6I/PA6ISO<sub>3</sub>)

Polyamides PA6I and PA6I/PA6ISO<sub>3</sub> were synthesized according to the protocol reported by Vannini et al. [9].

To synthesize PA6I, 24.92 g of IPA, 0.061 g of sodium hypophosphite as a catalyst, and 0.086 g of sodium acetate as an anti-crosslinker were combined in a round bottom flask. Subsequently, 20 mL of distilled water was added to suspend the solid monomers, and the mixture was stirred at 200 rpm. A solution of HDMA (17.43 g of HMDA dissolved in 20 mL of water) was then slowly dripped into the reactor for 10 min, with a further addition of 10 mL of water to rinse the drip funnel, all at room temperature. The reactor was then placed in a salt bath at 200  $^{\circ}$ C, and nitrogen was introduced to eliminate the water. The temperature was raised to 300  $^{\circ}$ C and after 150 min the product was withdrawn from the reactor. Finally the polyamide was crushed in a cryogenic mill, and stored in a sealed flask at room temperature.

In the synthesis of PA6I/PA6ISO $_3$ , IPA and 5-SIPA were employed as dicarboxylic reagents in a 80/20 M ratio, respectively, along with 17.43 g of HMDA as the diamine. 0.061 g of sodium hypophosphite, and 0.086 g of sodium acetate were incorporated. The process mirrored that of the PA6I synthesis; the polymer was discharged after 1 h. Scheme 3 depicts the synthesis reaction of poly(hexamethylene isophthalamide-co-5-sulfoisophthalamide).

2.2.3. Synthesis of the poly(ester-amide): poly(hexamethylene isophthalamide-co-5-sulfoisophthalamide-co-ricinoleic acid PA6I/PA6ISO $_3$ /PRA

In the synthesis of PA6I/PA6ISO $_3$ /PRA (Scheme 4), 17.43 g of HMDA, 19.96 g of IPA, 8.04 g of 5-SIPA, and 11.19 g of RA were used, maintaining the molar ratio IPA/5-SIPA/RA equal to 64/16/20.

Scheme 4. Synthesis of ionomeric copoly(ester-amide) poly(hexamethylene isophthalamide-co-5-sulfoisophthalamide-co-ricinoleic acid) (PA6I/PA6ISO<sub>3</sub>/PRA).

Additionally, 0.086 g of sodium acetate and 0.071 g of TBT were used. The process began at 190 °C. After collecting all the distilled water, the catalyst was added. Subsequently, the temperature was increased to 250 °C, and the vacuum was gradually applied. After 2 h, the temperature was raised to 270 °C and maintained for 3 h at 0.018 mbar, before collecting the polymer.

#### 2.3. Coating of PET films

A film coating was applied to bioriented PET films (23  $\mu m$  thick). Approximately 3 g of crushed PA6I/PA6ISO $_3$  was mixed with 7 g of distilled water, producing an opalescent solution after 15 min in an oven at 90 °C. The same process was carried out for PA6I/PA6ISO $_3$ /PRA, yielding a similar opalescent solution. To increase the superficial energy and improve the coating adhesion, the PET films were previously subjected to corona treatment. Then, the prepared solutions were applied onto PET films, using a Zehntner Automatic film applicator with a cylindrical bar, creating coatings with a nominal depth of 13.7  $\mu m$ .

Coating films with varying thicknesses of 3.8, 7.6, and 11.4  $\mu m$  were prepared by applying the aqueous polymer solution (30 % by weight) onto the PET substrate 1, 2, and 3 times, respectively. The characterization has been carried out on the thicker samples, and they were labeled PET<sub>PAGI/PAGISO3</sub> and PET<sub>PAGI/PAGISO3/PRA</sub>.

#### 2.4. Determination of cytotoxic activity

The cytotoxicity analysis was performed at the Biophotonics Group, São Carlos Institute of Physics, University of Sao Paulo. The films were previously sterilized in an autoclave at  $121\,^{\circ}\mathrm{C}$  for  $15\,\mathrm{min}$ . The cells viability was evaluated by means of a colorimetric assay using MTT 3-(4,5-dimethylthiazol-2-yl)-2,5-diphenyl tetrazolium bromide and a fibroblast culture (HDFn) through the material extract method in cell culture medium. As a control, an empty well of the culture plate was used. Data have been collected after 24 and 168 h.

#### 2.5. Determination of antibacterial activity

The strains Listeria monocytogenes Scott A, Escherichia coli ATCC 25922, Salmonella Enteritidis 155, and Staphylococcus aureus NCTC 10650, belonging to the microbial collection at the Department of Agricultural and Food Sciences, University of Bologna, were selected for this study. The strains were stored as 20 % glycerol stocks at  $-80\,^{\circ}$ C. Before use, the strains were revived and refreshed at least twice on Brain Heart Infusion (BHI, Oxoid, Basingstoke, UK).

The antimicrobial activity was assessed by measuring the survival rate of bacterial cells exposed to the prepared film samples. The four target microorganisms were cultivated aerobically in BHI medium for 16 h at 37  $^{\circ}$ C.

The resulting culture was centrifuged at 7000 rpm for 10 min, washed with sterile physiological saline solution (0.9 % w/v NaCl), and resuspended in the same solution to achieve a concentration of  $10^3$  colony-forming units (CFU) mL $^{-1}$ .

In accordance with the protocol described by Totaro et al. [16], the following film samples were tested: PET<sub>PA6I/PA6ISO3</sub> and PET<sub>PA6I/PA6ISO3/PRA</sub>. Segments of each sample, with a surface area of 2.5 cm², were precisely cut and placed into 2 mL tubes containing 1.5 mL of the previously prepared bacterial suspension. The tubes were incubated on a shaker at 100 rpm at room temperature (approximately 23  $\pm$  1 °C) for 24 h

Following incubation, each bacterial suspension underwent serial dilutions (1:10), which were subsequently plated onto the BHI medium. After incubating the plates at 37 °C for 24 h, the number of colonies, corresponding to the count of viable cells, was determined by averaging triplicate values. The reduction of viable cells, expressed as mortality percentage, was obtained through equation (1), reported by Lala et al. [28]:

$$Mortality \% = \frac{B - A}{B} * 100 \tag{1}$$

where A represents the mean number of viable cells following 24 h of exposure to the samples and B denotes the mean number of viable cells after 24 h of incubation in the absence of any material, serving as a positive control.

As the microbial content was found to be negligible for each sample, a negative control was not included.

#### 2.6. Characterizations

The inherent viscosities were measured at 30  $^{\circ}\text{C}$  with an Ubbelohde viscometer using a solution in phenol/1,1,2,2-tetrachloroethane (PhOH/TCE) 60/40 (wt/wt) at a concentration of 0.500  $\pm$  0.005 g/dL. Weight average molecular weight (Mw) and polydispersity index (PD) of PRA were determined using gel permeation chromatography (GPC) in CHCl $_3$  at ambient temperature on a HP 1100 Series apparatus with a PL gel 5  $\mu m$  Minimixed-C column with refractive index as detector. Polystyrene standards were used to prepare a universal calibration curve.

The  $^1$ H NMR spectra of PA6I, PRA, PA6I-PA6ISO $_3$  and copolymer PA6I/PA6ISO $_3$ /PRA were recorded at 600 MHz with a Varian Inova 600 spectrometer and were dissolved in a mixture of 1,1,1,3,3,3-hexafluoro-2-propanol/deuterated chloroform 50/50 (v/v), or just deuterated chloroform in case of PRA. The internal standard used as a reference was tetramethyl silane (TMS).

Thermogravimetric analysis (TGA) was performed using a PerkinElmer TGA4000 in a nitrogen atmosphere (40 mL min $^{-1}$ ) from 50 to 800  $^{\circ}\text{C}$  at a heating rate of 10  $^{\circ}\text{C}\text{-min}^{-1}$ .

Differential scanning calorimetry (DSC) was carried out using a PerkinElmer DSC6 under nitrogen flow (40 mL min $^{-1}$ ). The samples (PA6I and PA6I/PA6ISO $_3$ ) (around 10 mg) were first heated at  $20\,^{\circ}\text{C}\,\text{min}^{-1}$  from 20 to 280  $^{\circ}\text{C}$ , kept at this temperature for 1 min, and then cooled to  $20\,^{\circ}\text{C}$  at  $10\,^{\circ}\text{C}\,\text{min}^{-1}$ . After this, the samples were heated from 20  $^{\circ}\text{C}$  to 280  $^{\circ}\text{C}$  at  $10\,^{\circ}\text{C}\,\text{min}^{-1}$  (2nd scan). The same conditions were used for the copolymer (PA6I/PA6ISO $_3$ /PRA), but the minimum temperature reached in the cooling scan was  $-70\,^{\circ}\text{C}$ . The glass transition temperature (T $_g$ ) was determined during the 2nd heating scan: it was taken as the midpoint of the heat capacity increment associated with the glass-to-rubber transition.

Tensile properties were performed in a TA Instruments DMA Q800 equipment, with tension film type claws and dimensions of approximately  $5.2~\text{mm}\times6.3~\text{mm}\times0.75~\text{mm},$  with a frequency of 1 Hz, from 1 N min $^{-1}$  – 18 N, mode: force control and pre-load of 0.001 N.

#### 3. Results and discussions

This research builds on prior studies involving ionomeric polyamides [9] and antibacterial polyesters [16,17,23]. It was previously observed that the incorporation of a certain amount of ionomeric groups along the polymer chains, provided by 5-SIPA, imparts water solubility to the materials. The ionic groups (-SO<sub>3</sub>Na<sup>+</sup>) are expected to be randomly distributed along the chains, as all syntheses are conducted starting from monomers. The synthesis protocols for the polyamides (PA6I and PA6I/PA6ISO3) and polyester (PRA) presented here were based on previously published methods, confirming their reliability. In contrast, the poly(ester-amide) (PA6I/PA6ISO<sub>3</sub>/PRA), designed to explore its potential as an antimicrobial material, was prepared according to a protocol specifically developed in this study. Notably, the synthesis of the poly(ester-amide) was successful using only the catalyst specific for polyesterification. All syntheses proceeded efficiently; in particular the polyamide syntheses proceeded smoothly even without the need to apply a vacuum during the second stage of polycondensation.

PA6I, PA6I/PA6ISO $_3$ , and PRA were synthesized as reference materials. Specifically, the amount of sulfonated ionomeric groups along the

polymeric chain in PA6I/PA6ISO $_3$  was set at 20 mol% to ensure water solubility. Furthermore, to achieve an antibacterial effect in the material obtained from the combination of these components, it was deemed appropriate to incorporate a 20 mol% of ricinoleic acid (relative to 80 mol% of polyamides) in agreement with previous studies [16,17,23]. Additionally, to maintain the same proportion of sulfonated groups within the polyamide (i.e., 20 mol% of  $-SO_3^-Na^+$  groups), the molar ratio of the monomers in the PA6I/PA6ISO $_3$ /PRA was recalculated as follows: RA/HMDA/IPA/5-SIPA = 20/80/64/16.

#### 3.1. Synthesis and molecular characterization

The molecular structures of the homopolymers and copolymers were confirmed by  $^1$ H NMR analysis: Figs. 1–4 show the spectra obtained for PRA, PA6I, PA6I/PA6ISO $_3$  and PA6I/PA6ISO $_3$ /PRA.

Fig. 1 shows the spectrum of PRA, with signal assignments indicated by letters, which are also shown in the chemical structure on top. The precise assignment of each signal aligns with theoretical expectations based on the shielding effects of the nucleus due to the different chemical environments and it is consistent with findings previously reported by other authors [29]. Specifically, one can observe that at 0.9 ppm (t, 3H) resonate the protons k of the  $CH_3$  group, i.e., the more shielded nuclei of PRA, while at low field are located the two protons of vinyl unit (f and e) as well as the proton h, belonging to the carbon bound to ester functionality [16]. To dissolve the polyamide and poly (ester-amide) samples, it is necessary to first dissolve these materials in HFIP, a solvent that interacts with interchain polar bonds, weakening them, and then add CDCl3. The recorded NMR spectra thus exhibit a broad band between 3.8 and 5.2 ppm, attributed to the presence of HFIP. However, this band does not hinder the interpretation of the spectra, as the aliphatic signals resonate to its right, while the aromatic signals appear to its left. In particular, the spectrum of PA6I (Fig. 2) shows the signals at 3.5 ppm characteristic of the methylene protons *p* neighboring the amide group, and the signals related to protons q and r, at 2.0 and 1.5 ppm, respectively. On the other hands, at low fields resonate the deshielded nuclei, such as the aromatic ones (*l*, *m* and *n*) and the proton o linked to the nitrogen of the amide group [9].

Interestingly, the distinct structure of the sulfonated copolyamide  $PA6I/PA6ISO_3$  is clearly evident from the comparison of the spectrum

shown in Fig. 3: in the aromatic region, in addition to the disappearance of the signal corresponding to proton n, the splitting of the remaining signals (l, m and o) is observed. The protons on the sulfonated aromatic ring are labeled with a prime symbol and resonate at lower fields compared to their counterparts on the non-sulfonated ring. The direct comparison of the integrals of equivalent protons on the sulfonated and non-sulfonated units allows for the determination of the composition, reported in Table 2. Specifically, the ratio between the areas corresponding to protons m and m' indicates a molar composition of PA6I/PA6ISO $_3$  equal to 79/21, which closely aligns with the expected 80/20 ratio. Stars marked signals are due to the end groups.

Fig. 4 shows the  $^1$ H NMR spectrum recorded for PA6I/PA6ISO $_3$ /PRA, where the signals ascribable to the different PRA and PA6I units are evident.

In addition to the signals previously identified and discussed for the PRA, PA6I, and PA6ISO<sub>3</sub> units, the NMR spectrum of the poly(esteramide) reveals a new signal, labeled as o'', corresponding to the amidic proton o, which shifts to higher fields when directly bonded to the carbonyl group of ricinoleic acid. Furthermore, the appearance of a new signal centered at 2.2 ppm provides additional evidence for the incorporation of new units along the macromolecular chain. This resonance can be attributed both to the downfield deshielding of proton g upon esterification with the aromatic acids, and to the upfield shift of protons a, caused by the stronger shielding effect exerted by the amide functionality, formed through the reaction between the carboxylic group of PRA and the amine group of HMDA. No additional signals are detected, demonstrating the occurred copolymerization: the aromatic protons appear unaffected by bonding with the oxygen of ricinoleate, while proton h unfortunately overlaps with the HFIP band.

Nevertheless, the appearance of signal o'', and the change in the pattern of signals a, and g confirm the occurrence of copolymerization. The molar composition of the copolymer is calculated as the ratio between the normalized areas of the signals m, m', and k, which correspond to the PA6I, PA6ISO<sub>3</sub>, and PRA units, respectively.

The resulting molar composition was PA6I/PA6ISO<sub>3</sub>/PRA 66/18/16, approximating the nominal composition of 64/16/20, showing that less PA6I-PA6ISO<sub>3</sub> and more PRA were present with respect to the feed. Moreover, in the spectrum, the double bond around 5.5 ppm, referring to PRA, corresponds to 43 mol%, indicating that the polymerization

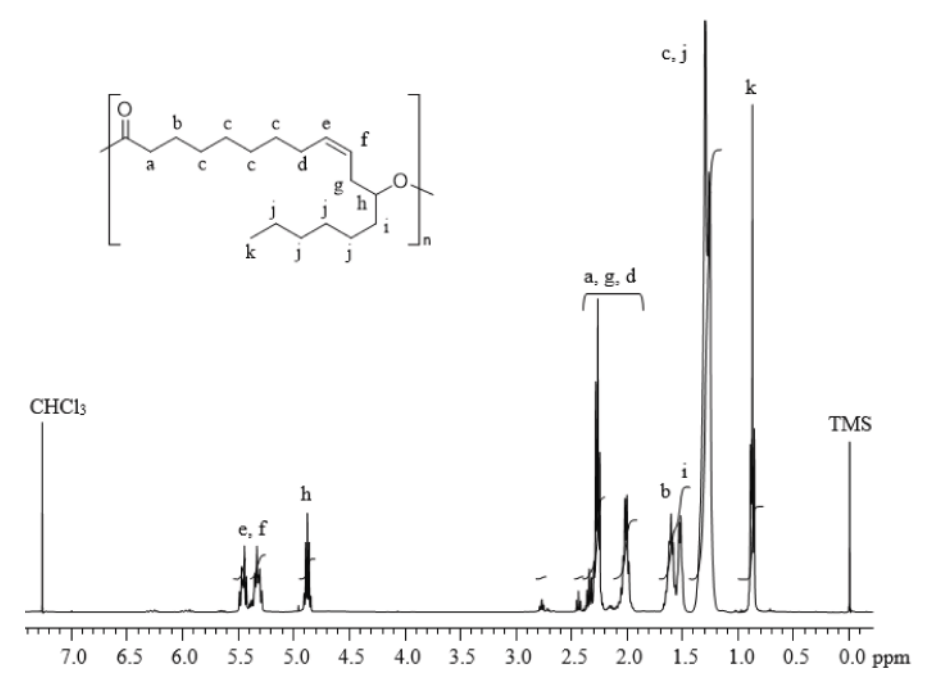


Fig. 1. <sup>1</sup>H NMR spectrum of PRA dissolved in CDCl<sub>3</sub>.

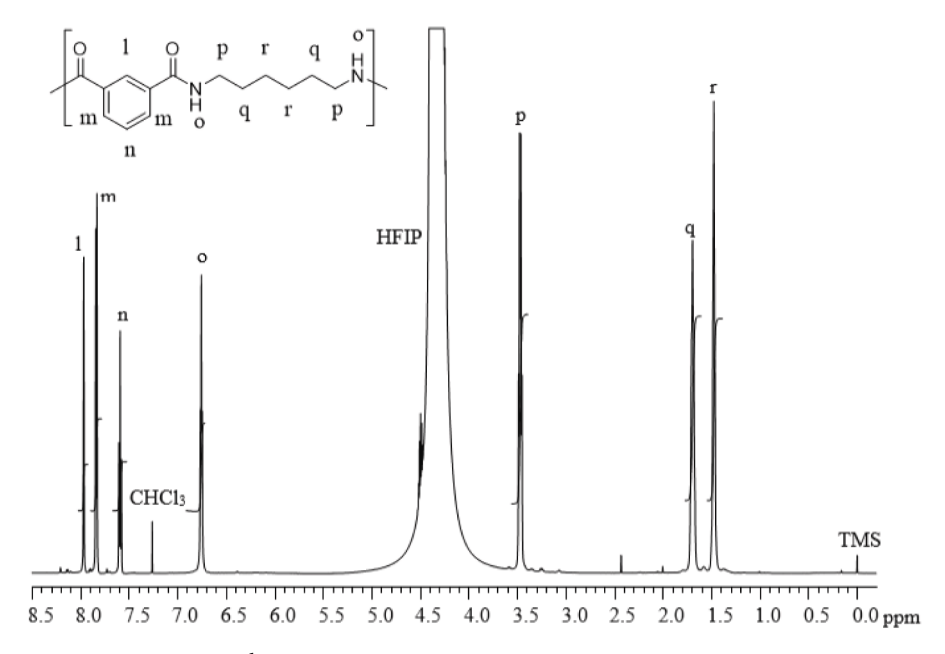


Fig. 2. <sup>1</sup>H NMR spectrum of PA6I dissolved in CDCl<sub>3</sub>/HFIP mixture.

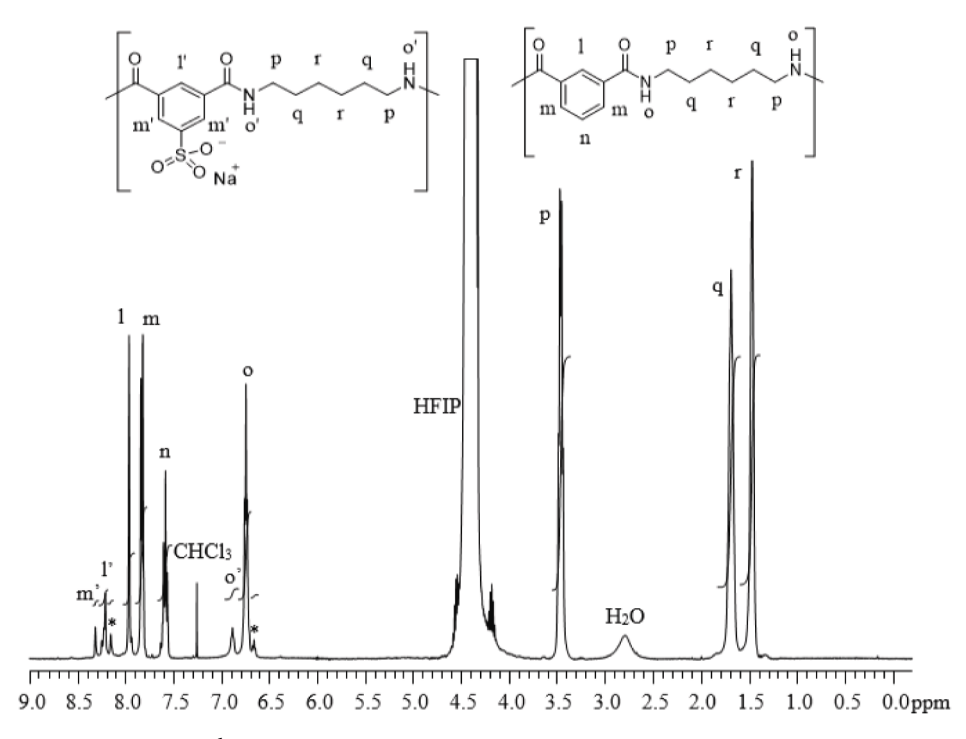


Fig. 3. <sup>1</sup>H NMR spectrum of PA6I/PA6ISO<sub>3</sub> dissolved in CDCl<sub>3</sub>/HFIP mixture.

process occurred with a decrement of the double bond. This decrease can be explained by the high reactivity of double bonds and the high temperature used during the copolymer synthesis, a fact also confirmed in studies on copolymers obtained from fatty acids of renewable sources [16,30,31].

The evaluation of the chain lengths of the obtained polymers through direct measurement via gel permeation chromatography (GPC) is not feasible due to the insolubility of polyamides in common GPC solvents. Therefore, to obtain a rough estimate of the extent of the polymerization process, the inherent viscosity was determined, which involves measuring the viscosity of polymer sample solutions at a defined concentration. The data obtained at 30 °C, presented in Table 2, indicate a

high viscosity for PA6I, while the viscosities for the copolyamide and the poly(estera-mide) are nearly halved. For reference, a PET bottle-grade polymer (*i.e.*, actual PET from a commercial bottle) exhibits an inherent viscosity of 0.74 under the same analytical conditions, whereas the PET film SARAFIL supplied by POLIPLEX and used later as a substrate for coating showed a viscosity of 0.56. In light of these comparative values, the results recorded gain clearer significance: both PA6I/PA6ISO<sub>3</sub> and PA6I/PA6ISO<sub>3</sub>/PRA are undoubtedly characterized by lower molecular weights, as also highlighted by the NMR analysis. In Figs. 3 and 4, which show the spectra of the copolyamide and poly(esteramide), the presence of signals corresponding to terminal units (starmarked) is evident, confirming that the obtained molecular weights are

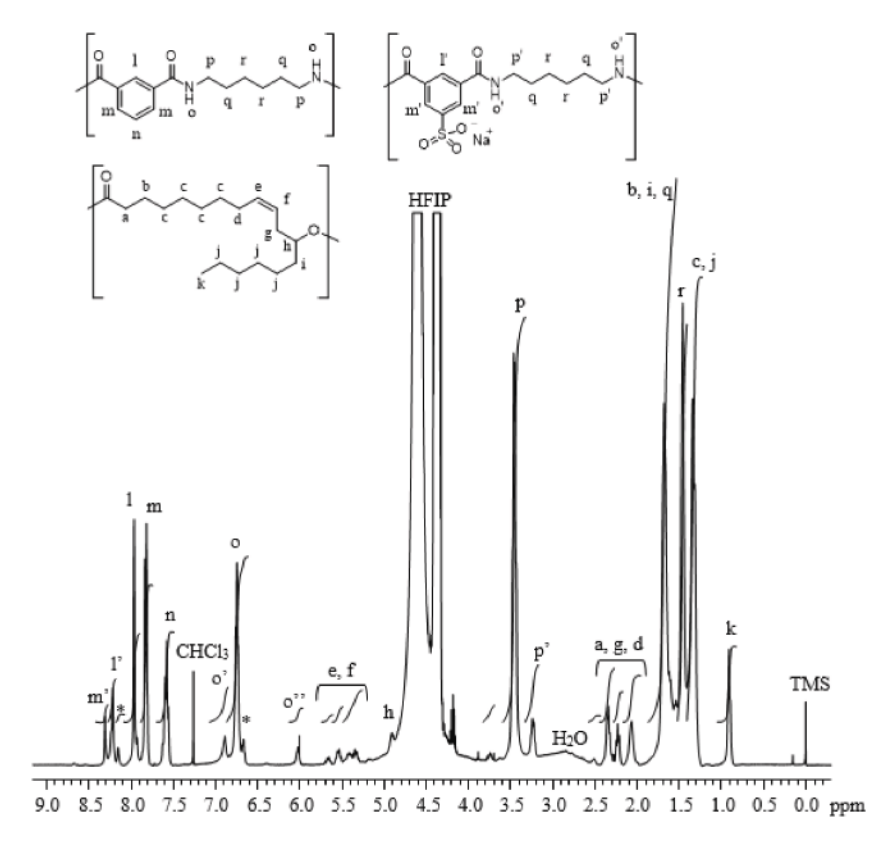


Fig. 4. <sup>1</sup>H NMR spectrum of PA6I/PA6ISO<sub>3</sub>/PRA dissolved in CDCl<sub>3</sub>/HFIP mixture.

**Table 2**Nominal and measured composition and inherent viscosity of polymers and copolymers.

Sample	Nominal ratio IPA/5- SIPA/RA (mol/mol/ mol)	Measured ratio IPA/5- SIPA/RA (mol/mol/ mol)	Inherent viscosity (dL/ g)
PRA	0/0/100	0/0/100	n.d. <sup>a</sup>
PA6I	100/0/0	100/0/0	0.60
PA6I/ PA6ISO <sub>3</sub>	80/20/0	79/21/0	0.31
PA6I/ PA6ISO <sub>3</sub> / PRA	64/16/20	66/18/16	0.31

<sup>&</sup>lt;sup>a</sup> Mw 17000 and polydispersity 3.8, determined by GPC in CHCl<sub>3</sub>.

not particularly high. Nonetheless, the samples, benefiting from polar interactions that effectively extend the apparent length of the polymer chains, are filmable and thus suitable for the intended coating application.

#### 3.2. Thermal analysis

Regarding thermal properties, Fig. 5 and Table 3 present the results of TGA and DSC of PA6I, PA6I/PA6ISO<sub>3</sub>, PA6I/PA6ISO<sub>3</sub>/PRA, and PRA for comparison purposes.

The findings indicate that PA6I and PA6I/PA6ISO $_3$  exhibited a single thermal decomposition step, whereas PRA and PA6I/PA6ISO $_3$ /PRA displayed a two-stage decomposition process (Fig. 5). The presence of the sulfonate group in the polyamide causes a marginal reduction in thermal stability. In the copoly(ester-amide), alongside the sulfonate group, the typical PRA structures also contribute to lowering the temperature at which decomposition initiates, as detailed in Table 3. Nevertheless, all materials demonstrate good thermal stability, with  $T_{onset}$  exceeding 340 °C, aligning with observations in other sulfonated

polymers [9,32,33]. The copolymer (PA6I/PA6ISO $_3$ /PRA) exhibiting a  $T_{onset}$  of 345  $^{\circ}$ C and two peaks at the maximum decomposition rate temperature of 380 and 469  $^{\circ}$ C, was selected for coating purposes. All samples were also characterized by DSC, and the derived data are listed in Table 3.

The DSC analysis indicates that, just like the poly(ricinoleic acid), the polyamide and the copolymer are amorphous. The glass transition temperature ( $T_g$ ) of the PA6I was  $122\,^{\circ}C$ , similar to the value reported in the literature [22,34,35]. The incorporation of the sulfonated group in the polyamide, PA6I/PA6ISO3, causes an increase in the  $T_g$  value, which goes to  $163\,^{\circ}C$ , a behavior also verified by Vannini et al. [9], who used the same proportion of polyamide/sulfonated group (80/20), and in studies with ionomeric polyesters and polysulfones [36,37]. This increase in  $T_g$  occurs due to intermolecular ionic interactions, where the sulfonated group acts as a sort of ionic cross-linker, reducing chain mobility and increasing  $T_g$ . However, different results were obtained by Bougarech et al. [38] and Zhi et al. [39] with ionomeric polyesters, where the  $T_g$  values decreased as the content of sulfonated groups increased. This can be explained by the large free volume occupied by the polymer chains.

The presence of RA units in the copolymer PA6I/PA6ISO $_3$ /PRA led to a slight decrease in the T $_g$  of the sulfonated polyamide due to the presence of the cis double bonds and the pendant chain of six aliphatic carbons in the RA unit. This justifies the decrease in the copolymer's T $_g$ . The T $_g$  of PRA was indeed  $-67~^{\circ}$ C. The data are coherent with the literature [9,16].

#### 3.3. Coating of poly(ester-amide)s on PET film

PA6I/PA6ISO $_3$  and PA6I/PA6ISO $_3$ /PRA were used as coatings for a commercially available PET film. The thicknesses of the resulting samples, namely PET<sub>PA6I/PA6ISO3</sub> and PET<sub>PA6I/PA6ISO3/PRA</sub>, were 3.8  $\mu$ m (one layer), 7.6  $\mu$ m (two layers), and 11.4  $\mu$ m (three layers), depending on the number of applications. All characterizations were performed with the

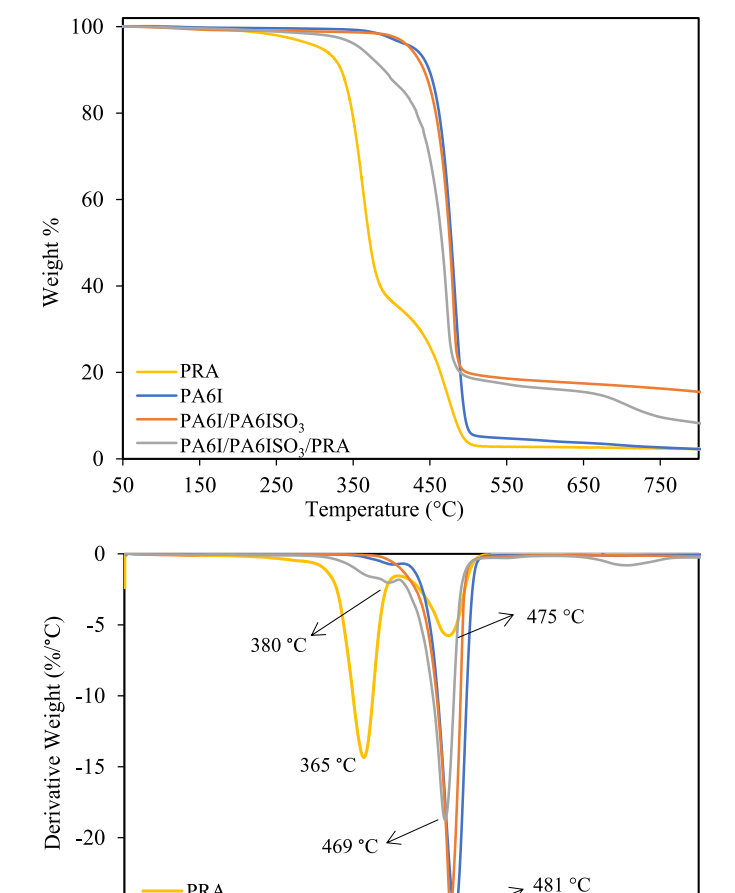


Fig. 5. TGA and dTGA curves of PRA, PA6I, PA6I/PA6ISO<sub>3</sub>, PA6I/PA6ISO<sub>3</sub>/ PRA under N2 atmosphere (40 mL/min).

Temperature (°C)

350

475

550

650

750

450

Table 3 Thermal data for PRA, PA6I, PA6I/PA6ISO<sub>3</sub>, PA6I/PA6ISO<sub>3</sub>/PRA.

Sample	TGA			DSC
	T <sub>onset</sub> <sup>a</sup> (°C)	T <sub>max</sub> <sup>b</sup> (°C)	T <sub>max</sub> <sup>c</sup> (°C)	T <sub>g</sub> (°C)
PRA	339	365	475	-67
PA6I	463	_	481	122
PA6I/PA6ISO <sub>3</sub>	457	_	475	163
PA6I/PA6ISO <sub>3</sub> /PRA	345	380	469	155

<sup>a</sup> initial thermal decomposition temperature.

PRA

PA6I

150

PA6I/PA6ISO<sub>3</sub>

PA6I/PA6ISO<sub>3</sub>/PRA

250

-25

-30

50

- $^{\rm b}$  maximum thermal decomposition rate temperature in the range 150–400  $^{\circ}\text{C}.$
- $^{
  m c}$  maximum thermal decomposition rate temperature in the range 400–600  $^{\circ}$ C.

thickest film.

#### 3.3.1. Mechanical properties of coated PET films

Fig. 6 shows the tensile strength at break, elongation at break, and Young's modulus for neat PET and the coated samples. Typical stressstrain curves are shown in Fig. 6d for PET, PET<sub>PA6I/PA6ISO3</sub>, and PET-

The findings show that adding both coatings improve tensile strength and elongation at break compared with the uncoated PET film. Young's modulus values indicate that  $\mbox{PET}_{\mbox{\scriptsize PA6I/PA6ISO3}}$  is stiffer than the pure PET. These improvements may be related to good interfacial compatibility between the coatings and the PET substrate, possibly involving

hydrogen bonding between the carbonyl groups along the PET chain (further activated by corona treatment) and the N-H groups of the amide functions in the PA6I segments of the copolymers, and interactions between hydrophobic regions of PET and the copolymer chains. However, additional analyses would be required to unambiguously confirm the underlying mechanism.

Indeed, corona treatment induces both chemical and physical modifications on the PET surface. The high-energy discharge generates surface radicals that react with atmospheric oxygen, leading to the introduction of polar functional groups such as hydroxyl, carbonyl, and carboxyl moieties. These new functionalities increase the surface energy and, consequently, improve wettability and adhesion to coatings or other materials [40,41]. In addition, the energetic bombardment can slightly increase surface roughness and remove organic contaminants, further enhancing interfacial interactions.

Taken together, these interactions are expected to contribute to the observed mechanical performance. At the industrial level, this is advantageous, as such materials may be processed in coating and laminating machines without the need for plasticizers due to their enhanced adhesion [9].

#### 3.3.2. Cytotoxicity analysis of coated PET films

Polymer films play a crucial role in wound dressings by promoting healing and preventing infection. To ensure they do not harm surrounding healthy tissue, it is essential that these films are non-cytotoxic [42]. Similarly, polymer films are widely used in food packaging to extend shelf life and maintain quality. In this context, non-cytotoxicity is critical to prevent the release of harmful substances into packaged food [43]. Therefore, to explore the potential applications of the materials under investigation, their cytotoxicity was assessed through fibroblast cell viability tests.

The results showed that although cell viability decreased in the 168h test compared to the 24-h test, all analyzed materials remained noncytotoxic compared to the control, Fig. 7, maintaining cell viability above 90 %, which is the threshold for a material to be considered not cytotoxic [44]. The PET film coatings (PET<sub>PA6I/PA6ISO3</sub> and PET<sub>PA6I/</sub> PA6ISO3/PRA) did not show cytotoxicity, similar to the uncoated PET film, contributing to cell viability rates above 90 %.

These findings are comparable with other type of coated PET: for example, Xv et al. [45] studied the cytotoxicity of hydrogels coating based on glycidyl methacrylate-phosphorylcholine-chitosan as a functionalizable anti-biofouling platform using commercial PET film as substrate. The Authors found that the coating had a cell viability between 90 and 110 %, while the uncoated PET film maintained a viability rate of 90 %.

#### 3.3.3. Antibacterial properties of coated PET films

The antibacterial properties of film samples against four bacterial strains of significant public health concern were investigated, namely Gram-positive Listeria monocytogenes Scott A and Staphylococcus aureus NCTC 10650, Gram-negative Salmonella Enteritidis 155 and Escherichia coli ATCC 25922. The antibacterial activity was evaluated based on the reduction in viable cells compared to a positive control.

The data reported in Table 4 indicate that the sample lacking PRA in its formulation, i.e., PET<sub>PA6I/PA6ISO3</sub>, did not display antibacterial activity against any of the bacteria tested. On the other hand, the sample containing ricinoleic acid units, i.e., PET<sub>PA6I/PA6ISO3/PRA</sub>, showed different mortality rates against L. monocytogenes and S. enteritidis, reaching 67.3 % and 41.9 % of mortality, respectively, after 24 h of exposure. However, the activity against E. coli was lower, around 23.1 %, while S. aureus was not susceptible to the tested film.

Although the highest mortality rate observed was nearly one log cycle, these findings are still noteworthy as they suggest different potential interactions between the bacteria and the tested films. The antibacterial effects may be due to "contact-killing" mechanisms or phenomena preventing bacterial adhesion. In general, most mechanisms

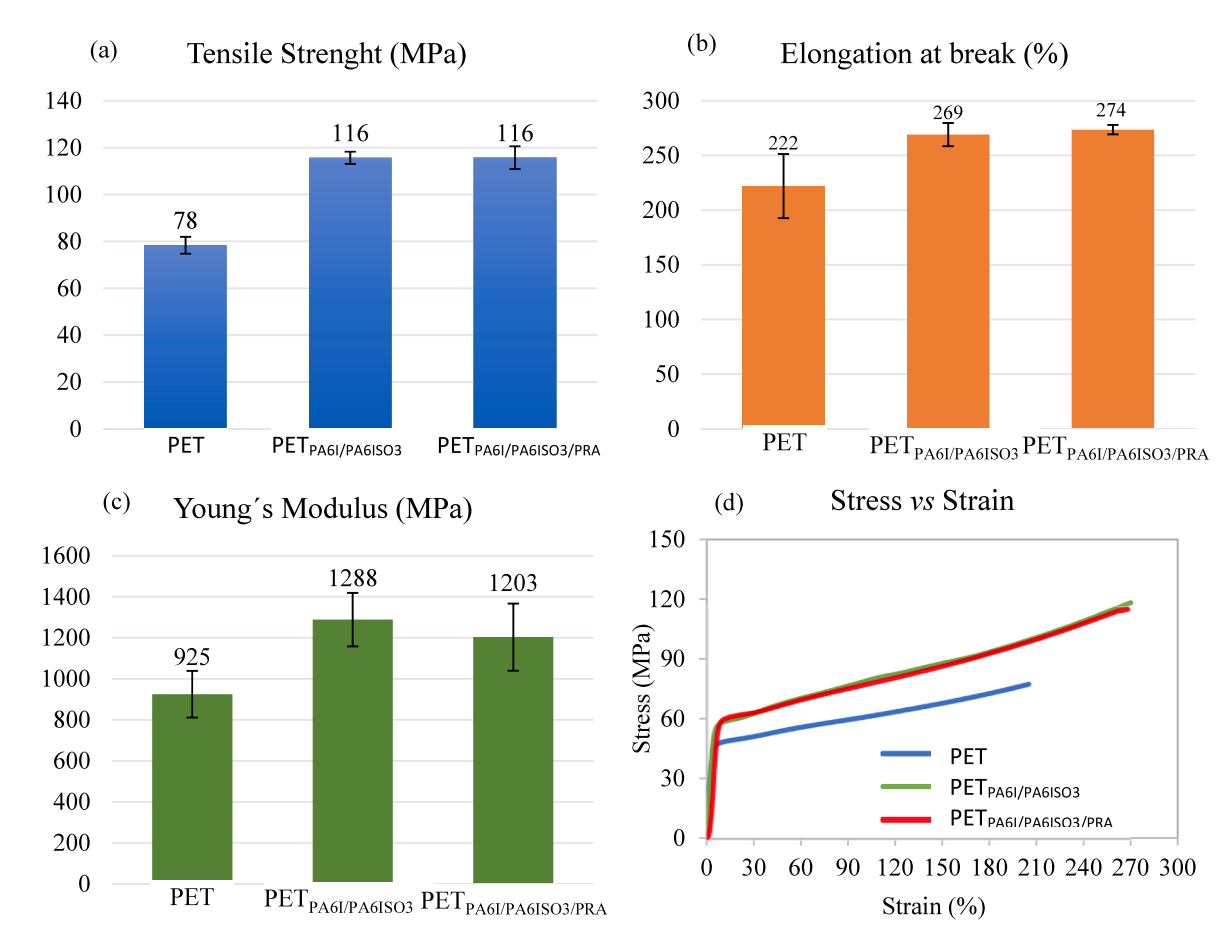


Fig. 6. Tensile strength at break a), elongation-at-break b), Young's Modulus c) and stress-strain curve d) for PET, PET PAGI/PAGISO3, and PETPAGI/PAGISO3/PRA-

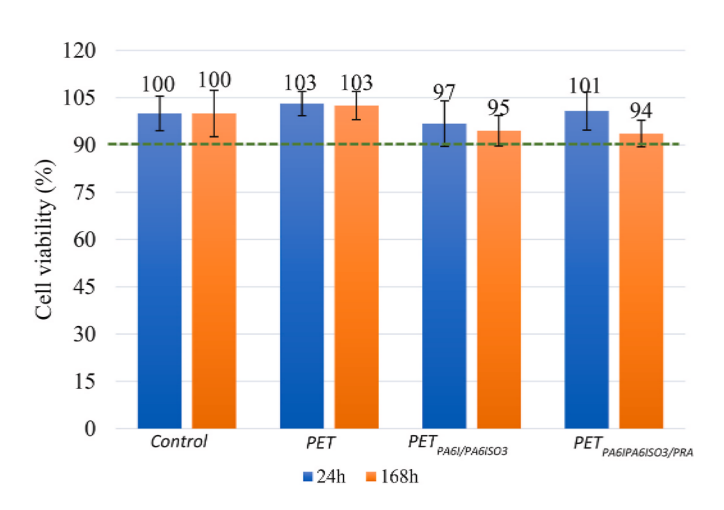


Fig. 7. Cell viability evaluated by MTT of PET, PET  $_{\rm PA6I/PA6ISO3,}$  and PET  $_{\rm PA6I/PA6ISO3/PRA,}$  after 24 and 168 h.

**Table 4** Antibacterial activity (expressed as mortality %) of PET<sub>PA6I/PA6ISO3</sub>, and PET-PA6I/PA6ISO3/PRA against four pathogenic bacterial strains, tested at level of  $10^3$  CFU  $mL^{-1}$ , after 24 h of exposure.

Sample	Mortality %			
	L. monocytogenes	S. aureus	S. enteritidis	E. coli
PET <sub>PA6I/PA6ISO3</sub>	$2.7\pm1.2$	$0.0\pm0.0$	$0.0\pm0.0$	$0.0\pm0.0$
PET <sub>PA6I/PA6ISO3/PRA</sub>	$67.3\pm10.4$	$0.0\pm0.0$	$41.9 \pm 8.4$	$23.1 \pm 5.4$

rely on "contact-killing", where adhered bacteria are eliminated due to physical disruption of their cell walls, thanks to the long tethering chains able to penetrate the microbial envelope, or to the alteration of the permeability and functionality of the cell membrane [46,47].

According to the results obtained, the highest mortality percentage was observed against *L. monocytogenes*, which has a thick (20–80 nm) outer cell wall composed of highly cross-linked layers of peptidoglycan, covalently bound to teichoic acids. Differently, the cell wall of Gramnegative *S. enteritidis* is thinner (5–10 nm) but more complex, with peptidoglycan surrounded by an outer membrane containing lipopoly-saccharide and some non-specific porins [48]. This structural difference could explain the lower mortality observed for *S. enteritidis* compared to *L. monocytogenes*.

Similarly, *E. coli* is a Gram-negative bacterium with an extra outer lipopolysaccharide membrane, which likely acts as a barrier limiting the penetration or uptake of antimicrobial compounds, as previously reported [16]. Although *S. aureus* is a Gram-positive bacterium (like *L. monocytogenes*), it presents a thick cell wall, composed of peptidoglycan highly cross-linked through species-specific peptide bridges. Moreover, according to the literature, *S. aureus* may have intrinsic resistance mechanisms that render the tested antimicrobial compounds ineffective, maybe by preventing the microbial attachment. It is also possible that a higher amount of PRA (16 mol% in the tested sample) is required to achieve effective activity against both *S. aureus* and *E. coli*, as previously reported in case of copolyesters containing ricinoleic acid units [17].

These findings highlight the potential of PRA-containing film coatings as effective antimicrobial materials against L. monocytogenes. However, to significantly increase the mortality rate up to 99.9 % (3 log cycles), future research should focus on optimizing these formulations by increasing the PRA content. Expanding its spectrum of activity and

enhancing its bactericidal effect could pave the way for the development of innovative antimicrobial materials for applications in food packaging, healthcare, and other fields requiring effective bacterial control.

#### 4. Conclusions

In this study, water-soluble poly(ester-amide)s containing ricinoleic acid units were synthesized and coated on PET surfaces. Water solubility was achieved by adding a proper amount (15 mol%) of sulfonate groups randomly distributed along the polymeric chains. Ricinoleic acid, known for its antimicrobial properties, was introduced to impart antibacterial activity to the final materials. All synthesized samples were found to be amorphous. The incorporation of sulfonate into the polyamide PA6I/PA6ISO $_3$  increased the T $_g$  value from 122  $^{\circ}\text{C}$  in PA6I to 163 °C, while, the introduction of ricinoleic acid units in the PA6I/ PA6ISO<sub>3</sub>/PRA copolymer led to a slight reduction in the T<sub>g</sub> of the sulfonated polyamide, imparting increased flexibility to the material. Thermogravimetric analysis revealed that all synthesized polymers exhibited high thermal stability, up to approximately 340 °C. PA6I/ PA6ISO3 and PA6I/PA6ISO3/PRA were coated on PET films, and their tensile properties were assessed. The coated films exhibited higher Young's moduli (around 1200-1300 MPa) and elongation-at-break (around 270 %) compared to the uncoated films, which had a Young's modulus around 900 MPa and an elongation-at-break around 200 %. These findings suggest good interfacial compatibility between the PET film and the coatings, indicating that the process is viable without the need of plasticizers. All prepared films were non-cytotoxic and favored cell viability both in the 24 h and 168 h tests, resulting biocompatible. Moreover, the PET-coated film containing PRA showed antibacterial activity against L. monocytogenes and S. enteritidis. Therefore, the poly (ester-amide)s here prepared displayed characteristics indicative of potential utility in packaging and coating applications, particularly within the medical sector, where controlling the bacterial growth is of high interest.

#### CRediT authorship contribution statement

Roberta L. de Paula: Writing – original draft, Investigation, Formal analysis, Data curation. Grazia Totaro: Writing – original draft, Supervision, Investigation, Formal analysis, Data curation. Elisabete Frollini: Writing – review & editing, Visualization, Supervision, Resources. Micaela Vannini: Visualization, Validation, Methodology, Formal analysis. Laura Sisti: Writing – review & editing, Supervision, Methodology, Conceptualization. Natália M. Inada: Formal analysis. Clara Maria Gonçalves de Faria: Formal analysis. Marianna Ciccone: Investigation. Francesca Patrignani: Writing – original draft, Investigation. Annamaria Celli: Resources, Project administration.

#### **Funding sources**

This work was supported by the Coordination for the Improvement of Higher Education Personnel (Brazil) (Financing Code 001).

#### Declaration of competing interest

The authors declare the following financial interests/personal relationships which may be considered as potential competing interests: Roberta L. de Paula reports financial support was provided by Coordination of Improvement of Higher Levels (Brazil) (Financing Code 001). If there are other authors, they declare that they have no known competing financial interests or personal relationships that could have appeared to influence the work reported in this paper.

#### Data availability

Data will be made available on request.

#### References

- [1] N. Upadhyay, S. Tripathi, A. Kushwaha, S.M. Bhasney, M. Mishra, Renewable bio-based materials: a journey towards the development of sustainable ecosystem, in: C.M. Hussain, A. Kushwaha, R.N. Bharagava, L. Goswami (Eds.), Bio-Based Materials and Waste for Energy Generation and Resource Management, Elsevier, 2023, pp. 31–75.
- [2] R. Balart, N. Montanes, F. Dominici, T. Boronat, S. Torres-Giner, Environmentally Friendly Polymers and Polymer Composites, first ed., MDPI, Basel, 2021.
- [3] M. Winnacker, B. Rieger, Poly (ester amide) s: recent insights into synthesis, stability and biomedical applications, Polym. Chem. 7 (46) (2016) 7039–7046.
- [4] S.D. Rajput, D.G. Hundiwale, P.P. Mahulikar, V.V. Gite, Fatty acids based transparent polyurethane films and coatings, Prog. Org. Coating 77 (9) (2014) 1360–1368.
- [5] P.M. Paraskar, R.D. Kulkarni, Synthesis of isostearic acid/dimer fatty acid-based polyesteramide polyol for the development of green polyurethane coatings, J. Environ. Polym. Degrad. 29 (2021) 54–70.
- [6] S. Nilawar, Q. Dasgupta, G. Madras, K. Chatterjee, Degradable poly (ester amide) s from olive oil for biomedical applications, Emerg. Mater. 2 (2019) 153–168.
- [7] S. Pramanik, J. Hazarika, A. Kumar, N. Karak, Castor oil based hyperbranched poly (ester amide)/polyaniline nanofiber nanocomposites as antistatic materials, Ind. Eng. Chem. Res. 52 (16) (2013) 5700–5707.
- [8] G.F. Hutter, Water-soluble rosin polyamide resins, U.S. Patent No. 5 (66) (1991) 331.
- [9] M. Vannini, P. Marchese, A. Celli, C. Lorenzetti, Synthesis and characterization of novel water-soluble polyamides with enhanced gas barrier properties, Ind. Eng. Chem. Res. 57 (45) (2018) 15254–15261.
- [10] G. Stoeppelmann, B. Hoffmann, B.N. Lamberts, U.S. Patent No 9 (631) (2017), 070.
- [11] J. Bariyanga, J.M.T. Johnson, E.M. Mmutlane, E.W. Neuse, A water-soluble polyamide containing cis-dicarboxylato-chelated platinum (II), J. Inorg. Organomet. Polym. Mater. 15 (2005) 335–340.
- [12] M. Bautista, A. Martinez de Ilarduya, A. Alla, S. Muñoz-Guerra, Poly (butylene succinate) ionomers with enhanced hydrodegradability, Polymers 7 (7) (2015) 1232–1247.
- [13] Y. Bai, L. Huang, T. Huang, J. Long, Y. Zhou, Synthesis and characterization of a water-soluble nylon copolyimide, Polymer 54 (16) (2013) 4171–4176.
- [14] Y.T. Yoo, B.J. Lee, S.I. Han, S.S. Im, D.K. Kim, Physical properties and biodegradation of poly (butylene adipate) ionomers, Polym. Degrad. Stabil. 79 (2) (2003) 257–264.
- [15] D.S. Ogunniyi, Castor oil: a vital industrial raw material, Bioresour. Technol. 97 (9) (2006) 1086–1091.
- [16] G. Totaro, L. Cruciani, M. Vannini, G. Mazzola, D. Di Gioia, A. Celli, L. Sisti, Synthesis of Castor oil-derived polyesters with antimicrobial activity, Eur. Polym. J. 56 (1) (2014) 174–184.
- [17] G. Totaro, L. Sisti, N.B. Cionci, G.A. Martinez, D. Di Gioia, A. Celli, Elastomeric/ antibacterial properties in novel random Ricinus communis based-copolyesters, Polym. Test. 90 (2020) 106719.
- [18] M.Y. Krasko, A.J. Domb, Hydrolytic degradation of ricinoleic-sebacic-esteranhydride copolymers, Biomacromolecules 6 (4) (2025) 1877–1884.
- [19] A. Shikanov, A.J. Domb, Poly (sebacic acid-co-ricinoleic acid) biodegradable injectable in situ gelling polymer, Biomacromolecules 7 (1) (2006) 288–296.
- [20] B. Vaisman, D.E. Ickowicz, E. Abtew, M. Haim-Zada, A. Shikanov, A.J. Domb, In vivo degradation and elimination of injectable ricinoleic acid-based poly (esteranhydride), Biomacromolecules 14 (5) (2013) 1465–1473.
- [21] A.R. Kelly, D.G. Hayes, Lipase-catalyzed synthesis of polyhydric alcohol-poly (ricinoleic acid) ester star polymers, J. Appl. Polym. Sci. 101 (3) (2006) 1646–1656.
- [22] A. Cassales, L.A. Ramos, E. Frollini, Synthesis of bio-based polyurethanes from Kraft lignin and Castor oil with simultaneous film formation, Int. J. Biol. Macromol. 145 (2020) 28–41.
- [23] G. Totaro, L. Paltrinieri, G. Mazzola, M. Vannini, L. Sisti, C. Gualandi, A. Ballestrazzi, S. Valeri, A. Pollicino, A. Celli, D. Di Gioia, L.M. Focarete, Electrospun fibers containing bio-based ricinoleic acid: effect of amount and distribution of ricinoleic acid unit on antibacterial properties, Macromol. Mater. Eng. 300 (11) (2015) 1085–1095.
- [24] S.B. Heo, Y.S. Jeon, S.I. Kim, S.H. Kim, J.H. Kim, Bioinspired adhesive coating on PET film for antifouling surface modification, Macromol. Res. 22 (2014) 203–209.
- [25] F. Seto, A. Kishida, Y. Muraoka, M. Akashi, Surface modification of poly (ethylene terephthalate) film by coating with poly (ethylene glycol)-grafted polystyrene, J. Appl. Polym. Sci. 74 (6) (1999) 1524–1530.
- [26] I. Azpitarte, G.A. Botta, C. Tollan, M. Knez, SCIP: a new simultaneous vapor phase coating and infiltration process for tougher and UV-resistant polymer fibers, RSC Adv. 10 (27) (2020) 15976–15982.
- [27] X. Chen, J. Zhou, J. Ma, Synthesis of a cationic fluorinated polyacrylate emulsifier-free emulsion via ab initio RAFT emulsion polymerization and its hydrophobic properties of coating films, RSC Adv. 5 (118) (2015) 97231–97238.
- [28] N.L. Lala, R. Ramaseshan, L. Bojun, S. Sundarrajan, R.S. Barhate, L. Ying-jun, S. Ramakrishna, Fabrication of nanofibers with antimicrobial functionality used as filters: protection against bacterial contaminants, Biotechnol. Bioeng. 97 (6) (2007) 1357–1365.
- [29] W.X. Wu, J. Li, X.L. Yang, N. Wang, X.Q. Yu, Lipase-catalyzed synthesis of renewable acid-degradable poly (β-thioether ester) and poly (β-thioether ester-coricinoleic acid) copolymers derived from Castor oil, Europ, Polym. J. 121 (2019) 109315.

- [30] P. Rämänen, S.L. Maunu, Structure of tall oil fatty acid-based alkyd resins and alkyd-acrylic copolymers studied by NMR spectroscopy, Prog. Org. Coating 77 (2) (2014) 361–368.
- [31] M. Black, J. Messman, J. Rawlins, Chain transfer of vegetable oil macromonomers in acrylic solution copolymerization, J. Appl. Polym. Sci. 120 (3) (2011) 1390–1396.
- [32] S. Banerjee, K.K. Kar, Impact of degree of sulfonation on microstructure, thermal, thermomechanical and physicochemical properties of sulfonated poly ether ether ketone, Polymer 109 (2017) 176–186.
- [33] A.A. Santiago, A. Ibarra-Palos, J.A. Cruz-Morales, J.M. Sierra, M. Abatal, I. Alfonso, J. Vargas, Synthesis, characterization, and heavy metal adsorption properties of sulfonated aromatic polyamides, High Perform. Polym. 30 (5) (2018) 591–601.
- [34] T. Cousin, J. Galy, A. Rousseau, J. Dupuy, Synthesis and properties of polyamides from 2, 5-furandicarboxylic acid, J. Appl. Polym. Sci. 135 (8) (2018) 45901.
- [35] Y.S. Hu, S. Mehta, D.A. Schiraldi, A. Hiltner, E. Baer, Effect of water sorption on oxygen-barrier properties of aromatic polyamides, J. Polym. Sci. B Polym. Phys. 43 (11) (2005) 1365–1381.
- [36] M. Bautista, , M., A.M. de Ilarduya, A. Alla, M. Vives, J. Morató, S. Muñoz-Guerra, Cationic poly (butylene succinate) copolyesters, Eur. Polym. J. 75 (2016) 329–342.
- [37] H.B. Park, H.S. Shin, Y.M. Lee, J.W. Rhim, Annealing effect of sulfonated polysulfone ionomer membranes on proton conductivity and methanol transport, J. Membr. Sci. 247 (1–2) (2005) 103–110.
- [38] A. Bougarech, S. Abid, M. Abid, Poly(ethylene 2, 5-furandicarboxylate) ionomers with enhanced liquid water sorption and oxidative degradation, J. Polym. Res. 27 (8) (2020) 1–10.
- [39] J. Zhi, B. Zhang, Y. Wu, Z. Feng, Study on a series of main-chain liquid–crystalline ionomers containing sulfonate groups, J. Appl. Polym. Sci. 81 (9) (2001) 2210–2218
- [40] M. Lindner, N. Rodler, M. Jesdinszki, M. Schmid, S. Sängerlaub, Surface energy of corona treated PP, PE and PET films, its alteration as function of storage time and

- the effect of various dosage on their bond strenght after lamination, J. Appl. Polym. Sci.  $135\ (11)\ (2018)\ 45842$ .
- [41] B. Das, D. Chakrabarty, C. Guha, S. Bose, Effects of corona treatment on surface properties of co-extruded transparent polyethylene film, Polym. Eng. Sci. 61 (5) (2021) 1449–1462.
- [42] R. Kesharwani, R. Yadav, S. Kesharwani, S. Tripathy, P. Verma, D.K. Patel, Polymer based biofilms: development and clinical application in medical science, Biomed. Mater. Dev 2 (1) (2024) 275–287.
- [43] A.G. Parente, H.P. de Oliveira, M.P. Cabrera, D.F. de Morais Neri, Bio-based polymer films with potential for packaging applications: a systematic review of the main types tested on food, Polym. Bull. 80 (5) (2023) 4689–4717.
- [44] B.R. Barrioni, S.M. de Carvalho, R.L. Orefice, A.A.R. de Oliveira, M. de Magalhaes Pereira, Synthesis and characterization of biodegradable polyurethane films based on HDI with hydrolyzable crosslinked bonds and a homogeneous structure for biomedical applications, Mater. Sci. Eng. C 52 (2015) 22–30.
- [45] J. Xv, H. Li, W. Zhang, G. Lai, H. Xue, J. Zhao, J, M. Tu, R. Zeng, R, Anti-biofouling and functionalizable bioinspired chitosan-based hydrogel coating via surface photo-immobilization, J. Biomater. Sci. Polym. Ed. 30 (5) (2019) 398–414.
- [46] M. Cloutier, D. Mantovani, F. Rosei, Antibacterial coatings: challenges, perspectives, and opportunities, Trends Biotechnol. 33 (11) (2015) 637–652.
- [47] S.G. Sanjeeva, S.K. Bajire, R.P. Shastry, R.P. Johnson, Antimicrobial coatings based on polymeric materials, in: A. Kumar, A. Behera, M. Bilal, R.K. Gupta, T.A. Nguyen (Eds.), Antiviral and Antimicrobial Smart Coatings: Fundamentals and Applications, Elsevier, 2023, pp. 309–355.
- [48] E. Sawosz, A. Chwalibog, J. Szeliga, F. Sawosz, M. Grodzik, M. Rupiewicz, M, T. Niemiec, K. Kacprzyk, Visualization of gold and platinum nanoparticles interacting with Salmonella enteritidis and Listeria monocytogenes, Int. J. Nanomed. 5 (2010) 631–637.